Atmospheric Flight Dynamic Simulation Modeling Of Spin-Stabilized Projectiles

Dimitrios N. Gkritzapis,[a] Elias E. Panagiotopoulos,[b] Dionissios P. Margaris[b] and Dimitrios G. Papanikas[b]

[a] Athens, Greece, GR 11522

[b] Fluid Mechanics Laboratory, Mechanical Engineering and Aeronautics Department, University of Patras, Patras, Greece, GR 26500

Abstract: *A full six degrees of freedom (6-DOF) simulation flight dynamics model is applied for the accurate prediction of short and long range trajectories of high and low spin-stabilized projectiles and small bullets via atmospheric flight to final impact point. The projectile is assumed to be both rigid (non-flexible), and rotationally symmetric about its spin axis launched at low and high pitch angles. The projectile maneuvering motion depends on the most significant forces and moment variations, in addition to wind and gravity. The computational flight analysis takes into consideration the Mach number and total angle of attack effects by means of the variable aerodynamic coefficients. For the purposes of the present work, linear interpolation has been applied taking data from official an tabulated database. The aforementioned variable flight model is compared with a trajectory atmospheric motion based on appropriate constant mean values of the aerodynamic projectile coefficients. Static stability, also called gyroscopic stability, is examined as a necessary condition for stable flight motion in order to determine the sufficient initial spinning projectile rotation. The efficiency of the method developed gives satisfactory results compared with published data of verified experiments and computational codes on atmospheric dynamics model flight analysis.*

Keywords: *Constant and variable aerodynamic coefficients, low and high launched angles, Magnus effects, symmetric projectiles dynamics, stability criteria, trajectory dynamics prediction*

Introduction

Ballistics is the science that deals with the motion of projectiles. The word ballistics was derived from the Latin 'ballista,' which was an ancient machine designed to hurl a javelin. The modern science of exterior ballistics[1] has evolved as a specialized branch of the dynamics of rigid bodies, moving under the influence of gravitational and aerodynamic forces and moments.

Pioneering English ballisticians Fowler, Gallop, Lock, and Richmond[2] constructed the first rigid six degrees of freedom projectile exterior ballistics model. Various authors have extended this projectile model for lateral force impulses[3,4] dual-spin projectiles[5,6] etc.

The present work addresses a full six degrees of freedom (6-DOF) flight dynamics analysis for accurate prediction of short and long-range trajectories of high spin-stabilized projectiles and small bullets. The proposed flight dynamic model takes into consideration the influence of the most significant forces and moment variations, in addition to wind and gravity forces. The variable aerodynamic coefficients are taken into account depending on the Mach number of flight and total angle of attack.

Additionally, this flight trajectory analysis is compared with another flight model based on appropriate constant mean values of the aerodynamic coefficients. The efficiency of the method developed gives satisfactory results compared with published data of verified experiments and computational codes on dynamics model flight analysis of short and long-range trajectories of spin-stabilized projectiles. The present analysis considers the cartridge 105 mm HE M1 with a 105 mm howitzer such as the M103 with M108 cannon, as a representative projectile type.

Projectile model

A typical formation of the Cartridge 105 mm HE M1 projectile is presented (see Figure 1), and is used with various 105 mm Howitzers (see Figure 2) such as US M49 with M52, M52A1

Figure 1. *105 mm HE M1 high explosive projectile artillery ammunition for howitzers.*

Figure 2. *Howitzer of 105 mm projectile at firing site.*

cannons, M2A1 & M2A2 with M101, M101A1 cannons, M103 with M108 cannon, M137 with M102 cannon as well as NATO L14 MOD56 and L5 (see Table 1).

Cartridge 105 mm HE M1 is a semi-fixed type ammunition, using adjustable propelling charges in order to achieve desirable ranges.

The projectile producing both fragmentation and blast effects can be used against personnel and materials targets. Technical characteristics and operational data of 105 mm HE M1 are illustrated (see Table 2).

Physicomathematical flight simulation model and simplifications

A six degrees of freedom rigid-projectile model [7–9,11] has three rotations and three translations, the three translation components (x,y,z) describing the position of the projectile's center of mass and the three Euler angles (ϕ,θ,ψ) describing the orientation of the projectile with respect to translation from the body frame (no-roll-frame, NRF, $\phi = 0$) to the plane fixed (inertial frame, if). For such flight bodies, the X_{NRF} axis of the projectile in the no-roll-frame coordinate system usually lies along the projectile axis of symmetry and the Y_{NRF} and Z_{NRF} axes are then oriented so as to complete a right-hand orthogonal system (Figure 3).

Table 1. *Maximum range impact of 105 mm HE M1 depending on cannon charge and muzzle velocity at firing site.*

Cannon charge	M52	M52A1, M101, M101A1	M102	M103
Cannon charge	1	7	1	7
Muzzle velocity/m s^{-1}	198.1	472.4	205.0	494.0
Maximum range/m	3510	11270	3700	11500

Table 2: *Technical characteristics and operational data limits of 105 mm HE M1 howitzer projectile.*

Technical description	Technical data
The cartridge 105 mm HE M1 consists	Total length: 790 mm
Projectile: Hollow steel forging	Total weight: 18.15 kg
High explosive charge: TNT (2.09 kg)	
Supplementary charge: TNT (0.14 kg)	Temperature limits:
Cartridge case: M14	Operation: −40 ºC to +52 ºC
Propelling charge: M67 (7 propelling charge increments)	Storage: −62 ºC to 71 ºC
Percussion primer: M28B2	
Fuse: PD M557P1 or equivalent	

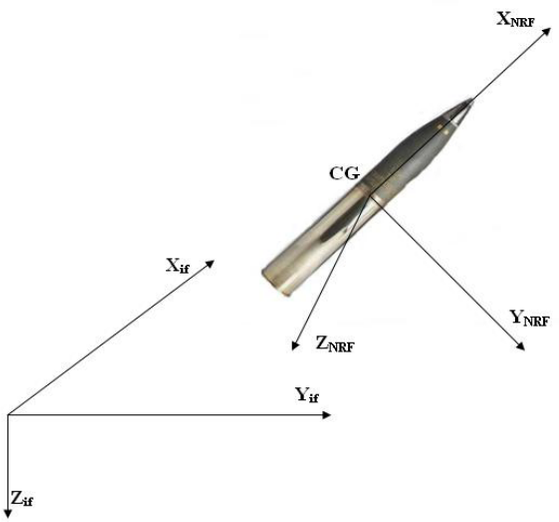

Figure 3. *No-roll (moving) and fixed (inertial) coordinate systems for the projectile trajectory analysis.*

Newton's laws of motion state that the rate of change of linear momentum must equal the sum of all the externally applied forces and the rate of change of angular momentum must equal the sum of all the externally applied moments, respectively. The force acting on the projectile comprises the weight W_f , the aerodynamic force A_f, and the Magnus force M_f.

The moment acting on the projectile comprises the moment due to the standard aerodynamic force A_m, the Magnus aerodynamic force M_m, and the unsteady aerodynamic moment UA_m. All aerodynamic coefficients are based on Mach number and the aerodynamic angles of attack and sideslip.

The independent variable is changed from time to dimensionless arc length and the equations that determine the pitching and yawing motion become independent of the size of the projectile which turns out to be very convenient in the analysis of free-flight range data.

The transformations to the no-roll-frame (~) give us equations (1)–(12).

$$x' = D\,\theta - \frac{D}{V}\,\psi\,\tilde{v} + \tilde{w}\,\theta\,\frac{D}{V} \tag{1}$$

$$y' = D\,\psi + \tilde{v}\,\frac{D}{V} + \tilde{w}\,\theta\,\psi\,\frac{D}{V} \tag{2}$$

$$z' = -D\,\theta + \frac{D}{V}\,\tilde{w} \tag{3}$$

$$\phi' = \frac{D}{V}\,\tilde{p} + \frac{D}{V}\,\tan|\theta|\,\tilde{r} \tag{4}$$

$$\theta' = \frac{D}{V}\,\tilde{q} \tag{5}$$

$$\psi' = \frac{D}{V\cos\theta}\,\tilde{r} \tag{6}$$

$$\tilde{u}' = -\frac{D}{V}\,g\,\theta - \frac{\pi}{8m}\rho V D^3 C_{D0} - D^3\,\frac{\pi}{8m}\rho V C_{D2}\,\frac{\tilde{w}^2}{V^2} - D^3\,\frac{\pi}{8m}\rho V C_{D2}\,\frac{\tilde{v}^2}{V^2} + \tilde{v}\,\frac{D}{V}\,\tilde{r} - \tilde{q}\,\frac{D}{V}\,\tilde{w} \tag{7}$$

$$\tilde{v}' = \; -D^3\,\frac{\pi}{8m}\rho V C_{NA}\,\frac{\tilde{v}}{V} + D^4\,\frac{\pi}{16m}\,\tilde{p}\rho C_{NPA}\,\frac{\tilde{w}}{V} + \frac{D}{V}\,\tilde{p}\,\tilde{w}\tan|\theta| - D\,\tilde{r} \tag{8}$$

$$\tilde{w}' = \frac{D}{V}\,g - D^3\,\frac{\pi}{8m}\rho V C_{NA}\,\frac{\tilde{w}}{V} - D^4\,\frac{\pi}{16m}\,\tilde{p}\rho C_{NPA}\,\frac{\tilde{v}}{V} + D\,\tilde{q} - \frac{D}{V}\,\tilde{p}\,\tilde{v} \tag{9}$$

$$\tilde{p}' = D^5 \frac{\pi}{16 I_{XX}} \tilde{p} \rho C_{LP} \tag{10}$$

$$\tilde{q}' = D^3 \frac{\pi}{8 I_{YY}} \rho V C_{NA} \frac{\tilde{w}}{V} LE_{MCP} + D^4 \frac{\pi}{16 I_{YY}} \rho C_{YPA} \tilde{p} \frac{\tilde{v}}{V} LE_{MCM} + \\ + D^5 \frac{\pi}{16 I_{YY}} \rho C_{MQ} \tilde{q} + D^4 \frac{\pi}{8 I_{YY}} \rho C_{MA} - \frac{D}{V} \tilde{r} \frac{I_{XX}}{I_{YY}} \tilde{p} - \frac{D}{V} \tilde{r}^2 \tan|\theta| \tag{11}$$

$$\tilde{r}' = -D^3 \frac{\pi}{8 I_{YY}} \rho V C_{NA} \frac{\tilde{w}}{V} LE_{MCP} + D^4 \frac{\pi}{16 I_{YY}} \tilde{p} \rho C_{YPA} \frac{\tilde{v}}{V} LE_{MCM} + \\ + D^5 \frac{\pi}{16 I_{YY}} \rho C_{MQ} \tilde{r} - D^4 \frac{\pi}{8 I_{YY}} \rho C_{MA} + \frac{D}{V} \tilde{p} \tilde{q} \frac{I_{XX}}{I_{YY}} + \frac{D}{V} \tilde{q} \tilde{r} \tan|\theta| \tag{12}$$

The projectile dynamic model consists of 12 highly first order non-linear ordinary differential equations, which are solved simultaneously by resorting to numerical integration using the fourth order Runge–Kutta method.

In these equations, the following sets of simplifications are employed: the aerodynamic angles of attack α, β are small so

$$\alpha \approx \tilde{w}/V, \beta \approx \tilde{v}/V$$

Also the yaw and pitch angles ψ, θ are small. A change of variables is to introduce velocity $\tilde{u}$ replaced by total velocity V because the side velocities $\tilde{v}$ and $\tilde{w}$ are also small. The Magnus force and moment are calculable quantities in comparison with the weight and aerodynamic forces so they are maintained in the forces and moments, respectively. The projectile is geometrically symmetrical so:

$$I_{XY} = I_{YZ} = I_{XZ} = 0 \quad \text{and} \quad I_{YY} = I_{ZZ}$$

The projectile is aerodynamically symmetric so the expressions of the distances from the center of mass to both the standard aerodynamic and Magnus centers of pressure are simplified.

Static or gyroscopic stability

Any spinning object will have gyroscopic properties. In a spin stabilized projectile, the center of pressure CP, the point at which the resultant air force is applied, is located in front of the center of gravity CG. Hence, as the projectile leaves the muzzle it experiences an overturning movement caused by air forces acting about the center of mass. It must be kept in mind that the forces are attempting to raise the projectile's axis of rotation.

In Figure 4 two cases of static stability are demonstrated: in the top figure, CP lies behind CG so that a clockwise (restoring) moment is produced. This case tends to reduce the yaw angle and return the body to its trajectory, therefore statically stable. Conversely, the lower figure, with CP ahead of CG, produces an anti-clockwise (overturning) moment which increases α further and is therefore statically unstable. It is also possible to have a neutral case in which CP and CG are coincident whereby no moment is produced.

There is clearly an important correspondence

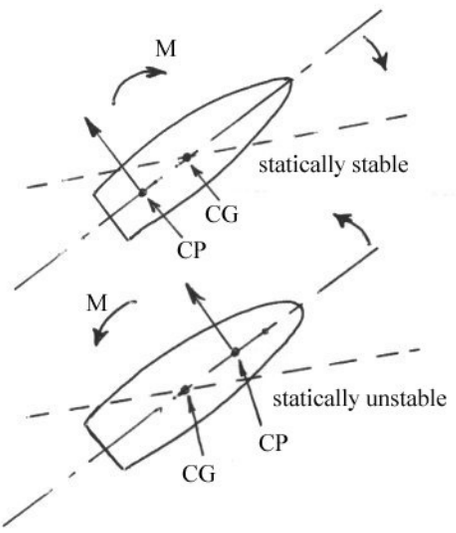

Figure 4. *Static stability/instability conditions.*

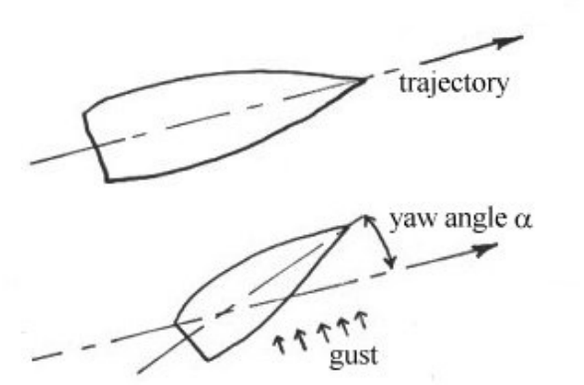

Figure 5. *Gust producing yaw angle on projectile in flight.*

between the distance from the centre of pressure to the centre of gravity and the static stability of the round. This distance is called the static margin. By definition, it is positive for positive static stability, zero for neutral stability and negative for negative stability.

Firstly, we shall consider the case of a shell-like projectile in flight (see Figure 5). This is initially flying at zero yaw incidence along its flight trajectory and is then struck by a gust of wind so that the nose is deflected upwards, producing a yaw angle (α). The response of the projectile to this disturbed yaw angle determines its stability characteristics. In particular, the initial response determines whether it is statically stable or unstable.

If the initial response is to move the nose back towards zero yaw (i.e. reducing the yaw angle) then it is statically stable. If the yaw angle initially increases as a response then it is statically unstable while if the disturbed yaw angle is retained the shell is neutral. It is therefore clear that it is the direction or sign of the resulting yawing moment generated that defines the static stability. This depends upon the aerodynamic force produced on the body due to the yaw angle and, in particular, upon the normal force (i.e. the aerodynamic force component perpendicular to the body axis) and the position at which it acts along the body's axis.

Classical exterior ballistics[10] defines the gyroscopic stability factor S_g, as:

Table 3. *Physical and geometrical characteristics of the 105 mm projectile.*

105 mm, HE, M1 projectile	
Reference diameter	104.8 mm
Projectile total length	49.47 cm
Projectile weight	15.00 Kg
Axial moment of inertia	0.02326 Kg m^2
Transverse moment of inertia	0.23118 Kg m^2
Center of gravity	18.34 cm from the base

Table 4. *Trajectory aerodynamic parameters of atmospheric flight dynamic model.*

105 mm, HE, M1 projectile with constant aerodynamic coefficients		
$C_D = 0.243$	$C_L = 1.76$	$C_{LP} = -0.0108$
$C_{MQ} = -9.300$	$C_{MA} = 3.76$	$C_{YPA} = -0.381$
$C_{NPA} = 0.215$		

$$S_g = \frac{I_X{}^2 \tilde{p}^2}{2\rho I_Y S d V^2 C_{MA}} \qquad (13)$$

The static factor is proportional to the product of four terms, which are the geometric technical characteristics of the projectile shape model, the square axial spin to velocity ratio, the aerodynamic Magnus effect variation and the proposed density atmospheric model.

This may be rearranged into:

$$S_g = \left(\frac{2 I_X{}^2}{I_Y \pi d^3}\right)\left(\frac{\tilde{p}^2}{V^2}\right)\left(\frac{1}{C_{MA}}\right)\left(\frac{1}{\rho}\right) \qquad (14)$$

The estimation of the projectile stability factor is effected from the last three terms separately, due to the fact that the first term is a constant parameter for a given projectile body motion.

Computational simulation

The flight dynamic model of the 105 mm HE, M1 projectile involves the solution of the set of the twelve non-linear first order ordinary differential equations (1)–(12) which are solved simultaneously

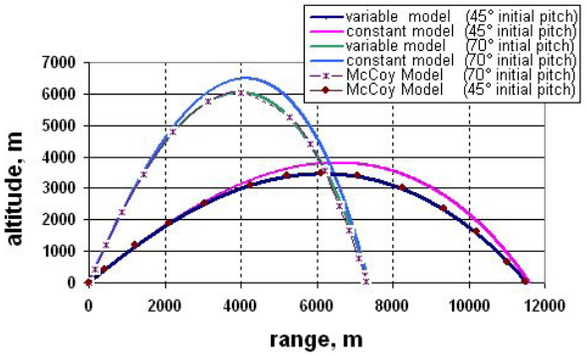

Figure 6. *Impact points and flight path trajectories with constant and variable aerodynamic coefficients for a 105 mm projectile compared with McCoy's trajectory data.*

by resorting to numerical integration using a fourth order Runge–Kutta method. Physical characteristics of the projectile 105 mm, HE, M1 are listed (see Table 3).

The constant dynamic flight model uses mean values of the experimental aerodynamic coefficient variations[1] (see Table 4).

For the trajectory parameters of the projectile with variable coefficients, linear interpolation has been applied taking data from the official tabulated database.[1] Initial data for both dynamic trajectory models with constant and variable aerodynamic coefficients are:

$x = 0.0$ m, $y = 0.0$ m, $z = 0.0$ m, $\phi = 0.0°$, $\theta = 45.0°$ and 70.0°, $\psi = 0.0°$, $\tilde{u}$ =494 m s^{-1}, $\tilde{v}$ = 0.0 m s^{-1}, $\tilde{w}$ = 0.0 m s−1, $\tilde{p}$ = 1644 rad s^{-1}, $\tilde{q}$ = 0.0 rad s^{-1} and $\tilde{r}$ = 0.0 rad s^{-1}. Giving the initial rifling twist rate η at the gun muzzle (calibers/turn) the axial spin rate is calculated from the expression:

$$\tilde{p} = 2\pi V / \eta D \quad (\text{rad s}^{-1}) \qquad (15)$$

The density and pressure are calculated as a function of altitude from the simple exponent model atmosphere, and gravity acceleration taken with the constant value $g = 9.80665$ m s^{-2}.

Results and discussion

The flight path trajectories of the present dynamic model with initial firing velocity of 494 m s^{-1} and rifling twist rate 1 turn in 18 calibers (1/18) of the M103 Howitzer at initial pitch angles of 45°

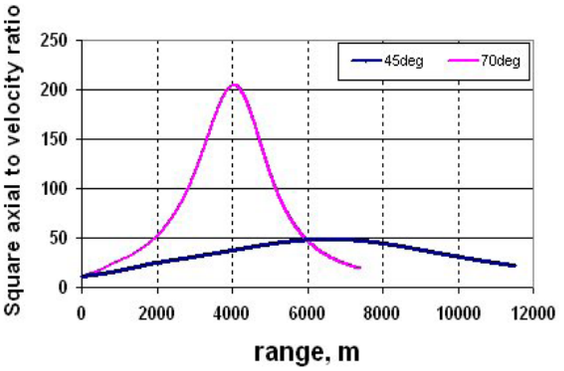

Figure 7. *Square axial spin to velocity ratio versus range at quadrant elevation angles of 45 and 70 degrees.*

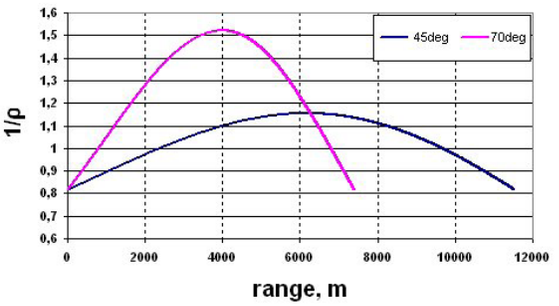

Figure 8. *Inverse of density versus range at quadrant elevation angles of 45 and 70 degrees for 105 mm projectile.*

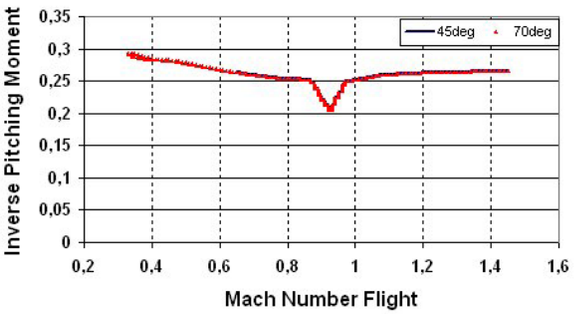

Figure 9. *Inverse pitching moment versus Mach number flight at quadrant angles of 45 and 70 degrees.*

and 70° are indicated in Figure 6 for two cases: constant and variable aerodynamic coefficients. The impact points of the above trajectories with the present variable coefficients method compared with accurate estimations of McCoy's flight atmospheric model[1] provide satisfactory agreement for the same conditions. The diagram shows that for the 105 mm M1 projectile, fired at sea-level with an angle of 45° (dark blue solid line) and no wind, the predicted range to impact is approximately 11 520 m, the time of flight is slightly greater than 53 s, and the maximum height is 3465 m. At 70° (green solid line), the predicted level-ground range is 7340 m, the time of flight to impact is about 72.5 s, and the maximum height is slight over 6030 m. In the same diagram, the basic differences from McCoy's flight data are remarked in trajectory models with constant aerodynamic coefficients.

The three final bracketed terms of the gyroscopic stability factor (equation (14)) contain trajectory variables which vary significantly during a projectile's flight and each will be considered independently below:

(a) Square axial spin to velocity ratio effect

The ratio of square axial spin to velocity (Figure 7) against range at 45°and 70° increases from a value of 11 at the muzzle, to values of 49 and 204 at the apogee, and then decreases to values of 22 and 19 at impact, respectively.

For the majority of projectiles, the velocity V will decay at a faster rate than the spin rate p. Consequently the launch conditions will be critical – S_g will increase (i.e. improve) as the projectile moves down-range.

It can be stated that if a projectile is statically stable at the muzzle, it will be statically stable for the rest of its flight. This we can understand because the static factor is proportional to the ratio of the projectile's rotational and transverse velocity. As the rotational velocity is much less damped than the transverse velocity (which is damped due to the action of the drag), the static factor increases, at least for the major part of the trajectory.

(b) Atmospheric density effect

The inverse of density against range at 45° and 70° (Figure 8) rises from 0.8 at the muzzle, to values

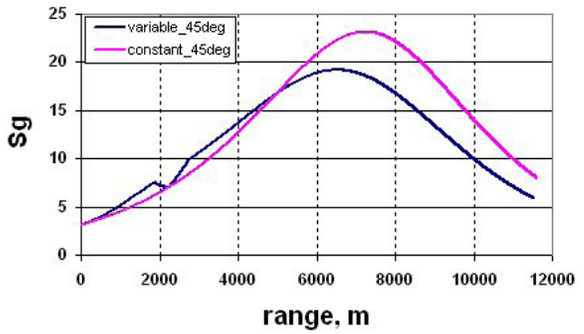

Figure 10. *Comparative static stability on the range with constant and variable coefficients at quadrant angle of 45 degrees.*

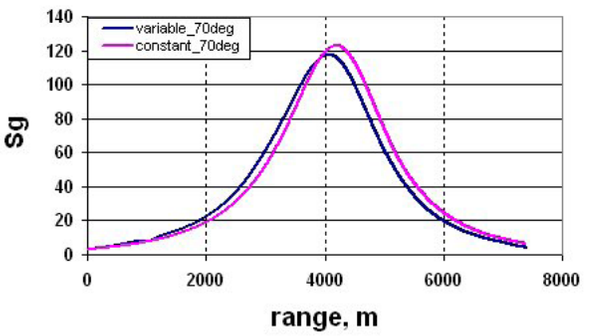

Figure 11. *Gyroscopic stability factor variations of constant and variable coefficients at 70 degrees initial pitch angle.*

of 1.15 and 1.52 at the apogee, and then decreases to a value of 0.8 at the point of impact.

Also S_g will be at its lowest when the density is at its highest. This will occur at low altitudes and at low temperature, high pressure atmospheric conditions. It is for this reason that firing trials for projectile impacts are often carried out in cold countries.

(c) Magnus aerodynamic effect

On the other hand the aerodynamic Magnus effect coefficient (Figure 9) clearly varies with anything which affects static margin. As a consequence, any variations in the positions of either CP or CG will directly affect the value of C_{MA}. The position of the CP will certainly vary during flight if the projectile

passes through the transsonic flow regime, due to complicated shock and expansion fan movements. In particular, it rises abruptly as the inverse C_{MA} term is highly reduced. This therefore means that S_g reduces under transsonic conditions.

The gyroscopic stability factor with constant and variable aerodynamic coefficients at 45° (Figure 10), which was 3.1 at the muzzle, increases to 23 and 19 at the summit of the trajectory and then decreases to values of 8 and 5.8 at impact, respectively. Also estimates of S_g have been made for aerodynamic coefficients with constant and variable values at 70° (Figure 11). It begins with an initial 3.1 at muzzle (the same value as at 45°), rising to 123 and 117 at the summit of the trajectory and then decreasing to values of 6.6 and 4.19 at the point of impact, respectively.

Conclusion

The six degrees of freedom (6-DOF) simulation flight dynamics model is applied for the accurate prediction of short and long range trajectories of high and low spin-stabilized projectiles and small bullets. It takes into consideration the Mach number and total angle of attack variation effects by means of the variable and constant aerodynamic coefficients. The criteria and analysis of gyroscopic stability are also examined. The computational results are in good agreement compared with other technical data and recognized projectile flight dynamic models.

References

1 R. L. McCoy, *Modern Exterior Ballistics*, Schiffer, Attlen, PA, 1999.

2 R. Fowler, E. Gallop, C. Lock and H. Richmond, The aerodynamics of spinning shells, *Philosophical Transactions of the Royal Society of London, Series A: Mathematical and Physical Sciences*, Vol. 221, 1920.

3 G. Cooper, Influence of yaw cards on the growth of spin stabilized projectiles, *Journal of Aircraft*, Vol. 38, No. 2, 2001, pp. 266–270.

4 B. Guidos and G. Cooper, Closed form solution of finned projectile motion subjected to a simple in-flight lateral impulse, *AIAA Paper* 2000-0767, 2000.

5 M. Costello and A. Peterson, Linear theory of a dual-spin projectile in atmospheric flight, *Journal of Guidance, Control, and Dynamics*, Vol. 23, No. 5, 2000, pp. 789–797.

6 B. Burchett, A. Peterson and M. Costello, Prediction of swerving motion of a dual-spin projectile with lateral pulse jets in atmospheric flight, *Mathematical and Computer Modeling*, Vol. 35, No. 1–2, 2002, pp. 1–14.

7 B. Etkin, *Dynamics of Atmospheric Flight*, John Wiley and Sons, New York, 1972.

8 L. C. Hainz and M. Costello, Modified Projectile Linear Theory for Rapid Trajectory Prediction, *Journal of Guidance, Control and Dynamics*, Vol. 28, No. 5, Sept–Oct 2005.

9 M. J. Amoruso, Euler Angles and Quaternions in Six Degree of Freedom Simulations of Projectiles, Technical Note, March 1996.

10 R. Nennstiel, How do Bullets Fly? *AFTE Journal*, Vol. 28, No. 2, April 1996.

11 M. F. Costello and D. P. Anderson, Effect of Internal Mass Unbalance on the Terminal Accuracy and Stability of a Projectile, *AIAA Paper* 96-3447, 1996.

Appendix – Equations of motion, forces and moment and symbols

The dynamic equations of motion are derived in the non-rolling frame and provided in equations (1) through (4):

$$\begin{Bmatrix} \overline{x}_{if} \\ \overline{y}_{if} \\ \overline{z}_{if} \end{Bmatrix} = \begin{bmatrix} \cos\theta\cos\psi & -\sin\psi & \sin\theta\cos\psi \\ \cos\theta\sin\psi & \cos\psi & \sin\theta\sin\psi \\ -\sin\theta & 0 & \cos\theta \end{bmatrix} \begin{Bmatrix} \tilde{u}_{NRF} \\ \tilde{v}_{NRF} \\ \tilde{w}_{NRF} \end{Bmatrix} \tag{1}$$

For position of the projectile and for orientation with Euler angles help

$$\begin{Bmatrix} \overline{\varphi} \\ \overline{\theta} \\ \overline{\psi} \end{Bmatrix} = \begin{bmatrix} 1 & 0 & t_\theta \\ 0 & 1 & 0 \\ 0 & 0 & 1/\cos\theta \end{bmatrix} \begin{Bmatrix} \tilde{p}_{NRF} \\ \tilde{q}_{NRF} \\ \tilde{r}_{NRF} \end{Bmatrix} \tag{2}$$

From the second law of Newton we have the force and the moment which act on the projectile in equations (3) and (4), respectively.

$$\begin{Bmatrix} \overline{\tilde{u}}_{NRF} \\ \overline{\tilde{v}}_{NRF} \\ \overline{\tilde{w}}_{NRF} \end{Bmatrix} = \begin{Bmatrix} \tilde{F}x_{TOTAL}/m \\ \tilde{F}y_{TOTAL}/m \\ \tilde{F}z_{TOTAL}/m \end{Bmatrix} + \begin{bmatrix} 0 & \tilde{r}_{NRF} & -\tilde{q}_{NRF} \\ -\tilde{r}_{NRF} & 0 & -\tilde{r}_{NRF}\, t_\theta \\ \tilde{q}_{NRF} & \tilde{r}_{NRF}\, t_\theta & 0 \end{bmatrix} \begin{Bmatrix} \tilde{u}_{NRF} \\ \tilde{v}_{NRF} \\ \tilde{w}_{NRF} \end{Bmatrix} \tag{3}$$

$$\left[I^{-1}\right]\left(\begin{Bmatrix} \tilde{L}_{TOTAL} \\ \tilde{M}_{TOTAL} \\ \tilde{N}_{TOTAL} \end{Bmatrix} - \begin{bmatrix} 0 & -\tilde{r}_{NRF} & \tilde{q}_{NRF} \\ \tilde{r}_{NRF} & 0 & \tilde{r}_{NRF}\, t_\theta \\ -\tilde{q}_{NRF} & -\tilde{r}_{NRF}\, t_\theta & 0 \end{bmatrix} \begin{bmatrix} I_{XX} & I_{XY} & I_{XZ} \\ I_{YX} & I_{YY} & I_{YZ} \\ I_{ZX} & I_{ZY} & I_{ZZ} \end{bmatrix} \begin{Bmatrix} \tilde{p}_{NRF} \\ \tilde{q}_{NRF} \\ \tilde{r}_{NRF} \end{Bmatrix} \right) \tag{4}$$

The force acting on the projectile in equation (3) comprises the weight W_f, the aerodynamic force A_f and Magnus force M_f:

$$\begin{Bmatrix} \tilde{F}x_{TOTAL} \\ \tilde{F}y_{TOTAL} \\ \tilde{F}z_{TOTAL} \end{Bmatrix} = \begin{Bmatrix} \tilde{X}w_f \\ \tilde{Y}w_f \\ \tilde{Z}w_f \end{Bmatrix} + \begin{Bmatrix} \tilde{X}_{Af} \\ \tilde{Y}_{Af} \\ \tilde{Z}_{Af} \end{Bmatrix} + \begin{Bmatrix} \tilde{X}_{Mf} \\ \tilde{Y}_{Mf} \\ \tilde{Z}_{Mf} \end{Bmatrix} \tag{5}$$

The moment acting on the projectile in equation (4) comprises the moment due to the standard aerodynamic force A_m, due to the Magnus aerodynamic force M_m and the unsteady aerodynamic moment UA_m:

$$\begin{Bmatrix} \tilde{L}_{TOTAL} \\ \tilde{M}_{TOTAL} \\ \tilde{N}_{TOTAL} \end{Bmatrix} = \begin{Bmatrix} \tilde{L}_{Am} \\ \tilde{M}_{Am} \\ \tilde{N}_{Am} \end{Bmatrix} + \begin{Bmatrix} \tilde{L}_{Mm} \\ \tilde{M}_{Mm} \\ \tilde{N}_{Mm} \end{Bmatrix} + \begin{Bmatrix} \tilde{L}_{UAm} \\ \tilde{M}_{UAm} \\ \tilde{N}_{UAm} \end{Bmatrix} \tag{6}$$

All aerodynamic coefficients are based on the Mach number and the aerodynamic angles of attack and sideslip:

$$\alpha = \tan^{-1}\left(\frac{\tilde{w}_{NRF}}{\tilde{u}_{NRF}}\right) \tag{7}$$

$$\beta = \tan^{-1}\left(\frac{\tilde{v}_{NRF}}{\tilde{u}_{NRF}}\right) \tag{8}$$

The total aerodynamic is velocity given in equation (9):

$$V_T = \sqrt{\tilde{u}_{NRF}{}^2 + \tilde{v}_{NRF}{}^2 + \tilde{w}_{NRF}{}^2} \tag{9}$$

The weight force in the no-roll system is:

$$\begin{Bmatrix} \tilde{X}w_f \\ \tilde{Y}w_f \\ \tilde{Z}w_f \end{Bmatrix} = mg \begin{Bmatrix} -\sin\theta \\ 0 \\ \cos\theta \end{Bmatrix} \tag{10}$$

The aerodynamic force, which acts on the projectile at the aerodynamic center of pressure, is:

$$\begin{Bmatrix} \tilde{X}_{Af} \\ \tilde{Y}_{Af} \\ \tilde{Z}_{Af} \end{Bmatrix} = \frac{1}{2}\rho V_T{}^2 S_{ref} \begin{vmatrix} -C_{X0} - C_{X2}\dfrac{\tilde{w}_{NRF}{}^2}{V_T{}^2} - C_{X2}\dfrac{\tilde{v}_{NRF}{}^2}{V_T{}^2} \\ -C_{NA}\dfrac{\tilde{v}_{NRF}}{V_T} \\ -C_{NA}\dfrac{\tilde{w}_{NRF}}{V_T} \end{vmatrix} \tag{11}$$

The Magnus force, which acts on the projectile at the Magnus force center of pressure, is:

$$\begin{Bmatrix} \tilde{X}_{Mf} \\ \tilde{Y}_{Mf} \\ \tilde{Z}_{Mf} \end{Bmatrix} = \frac{1}{2}\rho V_T{}^2 S_{ref} \begin{vmatrix} 0 \\ \dfrac{\tilde{p}_{NRF} D\, C_{\mathrm{NPA}} \tilde{w}_{NRF}}{2V_T{}^2} \\ \dfrac{-\tilde{p}_{NRF} D\, C_{\mathrm{NPA}} \tilde{v}_{NRF}}{2V_T{}^2} \end{vmatrix} \tag{12}$$

The moment due to the aerodynamic force is:

$$\begin{Bmatrix} \tilde{L}_{Ah} \\ \tilde{M}_{Ah} \\ \tilde{N}_{Ah} \end{Bmatrix} = \begin{bmatrix} 0 & 0 & 0 \\ 0 & 0 & -R_{\oplus MAC} \\ 0 & R_{\oplus MAC} & 0 \end{bmatrix} \begin{bmatrix} \tilde{X}_{Af} \\ \tilde{Y}_{Af} \\ \tilde{Z}_{Af} \end{bmatrix} \tag{13}$$

The moment due to the Magnus force is:

$$\begin{Bmatrix} \tilde{L}_{Mf} \\ \tilde{M}_{Mf} \\ \tilde{N}_{Mf} \end{Bmatrix} = \begin{bmatrix} 0 & 0 & 0 \\ 0 & 0 & -R_{\oplus MAX} \\ 0 & R_{\oplus MAX} & 0 \end{bmatrix} \begin{bmatrix} \tilde{X}_{Mf} \\ \tilde{Y}_{Mf} \\ \tilde{Z}_{Mf} \end{bmatrix} \tag{14}$$

In addition, for the unsteady moment UA_m is:

$$\begin{Bmatrix} \tilde{L}_{body} \\ \tilde{M}_{body} \\ \tilde{N}_{body} \end{Bmatrix} = \frac{1}{2}\rho V_T^{\,2} D^{S_{ref}} \begin{vmatrix} \dfrac{\tilde{p}_{NRF} DC_{LP}}{2V} \\ \dfrac{\tilde{q}_{NRF} DC_{MQ}}{2V} + \dfrac{C_{MA}}{V} \\ \dfrac{\tilde{r}_{NRF} DC_{MQ}}{2V} - \dfrac{C_{MA}}{V} \end{vmatrix} \qquad (15)$$

Forces and moments

Axial force = $\frac{1}{2}\rho V^2 S_{ref} C_x$

C_x = axial force coefficient

Normal force = $\frac{1}{2}\rho V^2 S_{ref} C_{NA}$

C_{NA} = normal force coefficient

Magnus force = $\frac{1}{2}\rho V^2 S_{ref} \left(\frac{pd}{V}\right) C_{NPA}$

C_{NPA} = Magnus force coefficient

Pitch damping moment =

$$\frac{1}{2}\rho V^2 S_{ref}\, d \left(\frac{q_t\, d}{V}\right)\left(C_{MQ} + C_{M\dot{a}}\right)$$

C_{MQ} : $coefficient\ due\ to\ q_t = \sqrt{q^2 + r^2}$, $total\ transverse\ angular\ velocity$

$C_{M\dot{a}}$: $coefficient\ due\ to\ \dot{a}_t = \frac{d\,a_t}{dt}$, $rate\ of\ change\ of\ total\ yaw\ angle$

Roll damping moment =

$$\frac{1}{2}\rho V^2 S_{ref}\, d \left(\frac{p\, d}{V}\right) C_{LP}$$

C_{LP} = roll damping moment coefficient

Magnus moment = $\frac{1}{2}\rho V^2 S_{ref}\, d \left(\frac{p\, d}{V}\right) C_{YPA} \sin a_t$

C_{YPA} = Magnus moment coefficient

Pitch or overturning moment =

$$\frac{1}{2}\rho V^2 S_{ref}\, d\, C_{MA} \sin a_t$$

C_{MA} = pitch or overturning moment coefficient

List of symbols

C_{X0}	zero-yaw axial aerodynamic coefficient
C_{X2}	square yaw axial aerodynamic coefficient
C_L	lift aerodynamic coefficient
C_{LP}	roll damping aerodynamic coefficient
C_{MQ}	pitch damping aerodynamic coefficient
C_{MA}	pitch moment coefficient

C_{YPA}	Magnus moment coefficient
C_{NPA}	Magnus force aerodynamic coefficient
$\bar{x}_{if}, \bar{y}_{if}, \bar{z}_{if}$	projectile position, in inertial space
$\tilde{u}_{NRF}, \tilde{v}_{NRF}, \tilde{w}_{NRF}$	projectile velocity components, expressed in no-roll-frame
$\tilde{p}_{NRF}$	projectile roll rate, expressed in no-roll-frame
$\tilde{q}_{NRF}, \tilde{r}_{NRF}$	projectile pitch and yaw rates expressed in no-roll-frame
$\bar{\theta}, \bar{\psi}$	projectile pitch and yaw angles
$\bar{\phi}$	projectile roll angle
I	projectile inertia matrix
I_{XX}, I_{YY}, I_{ZZ}	diagonal components of the inertia matrix
I_{XY}, I_{YZ}, I_{XZ}	off-diagonal components of the inertia matrix
V	total aerodynamic velocity
ρ	atmospheric density
S_{ref}	projectile reference area ($\pi d2/4$)
m	mass of projectile
t	time
α, β	aerodynamic angles of attack and sideslip
$R_{\oplus MAC}$	vector from the projectile center of mass to the center of pressure
$R_{\oplus MAX}$	vector from the projectile center of mass to the Magnus center of pressure
D	projectile reference diameter
g	gravity